

PHOTOMETRIC DECOMPOSITION OF THE MULTIPLE-NUCLEUS GALAXY NGC 6166

TOD R. LAUER

Princeton University Observatory

Received 1986 February 25; accepted 1986 May 14

ABSTRACT

The complex morphology of the multiple-nucleus cD galaxy NGC 6166 can be modeled as the line-of-sight superposition of two normal elliptical galaxies, B and C, against a central cD galaxy. Surface photometry profiles are measured for each component by a simultaneous isophote fitting algorithm. Galaxy B has a truncated brightness profile which may reflect a past close encounter with galaxy A. Further, a faint elongated feature is visible between galaxies B and C which may be a dynamical friction wake induced by the passage of galaxy C through the cD. No asymmetric tidal distortions of the galaxies are seen, however, nor are any other tidal features visible in the decomposition residual image; neither galaxy B or C appears to have passed as close to the cD as their projected radii. Galaxies B and C have normal velocity dispersions, cores, and effective radii for their luminosities when compared to other galaxies within the inner 1 Mpc of A2199, the cluster containing NGC 6166. These galaxies appear to be members of the central population of A2199 which may have occasional high velocity encounters with the central cD galaxy but do not appear to be residual cores of much more luminous galaxies strongly cannibalized by the cD.

Subject headings: galaxies: clustering — galaxies: individual — galaxies: nuclei — galaxies: photometry

I. INTRODUCTION

Photometric image decomposition of multiple-nucleus first-ranked cluster galaxies offers a direct approach towards untangling their structure and origin. If these systems are direct evidence for the galactic cannibalism model of cD formation proposed by Hausman and Ostriker (1978), then image analysis may reveal strong tidal effects on their less luminous secondary nuclei, which would be the remains of cluster galaxies presently merging with their central galaxies. Isophotes around the nuclei might be sheared, distorted, or drawn out into tidal plumes; the nucleus of the cD might be disturbed by the close approach of the dense cores of cannibalized galaxies. Tidal stripping of stars from the infalling galaxies might cause them to deviate from luminosity-dependent parameter relationships for normal galaxies. Some recent investigators, however, have questioned the formation of first-ranked galaxies by cannibalism. Merritt (1984*a*) argues that dynamical friction in rich clusters is too weak to pull enough cluster galaxies into the core over the age of the universe to produce cD galaxies. Further, the radial velocities of the secondary nuclei relative to their central galaxies are often too high for them to be bound systems (Tonry 1984). Merritt (1984*b*) and Tonry (1985) both propose cluster dynamics and evolution scenarios that would create line-of-sight enhancements of galaxies around central cD galaxies to account for the high 25%–50% frequency occurrence of multiple-nucleus first-ranked galaxies in clusters observed by Hoessel (1980) and Schneider, Gunn, and Hoessel (1983*a*). Under this picture, most multiple systems are simply the projected superposition of normal cluster galaxies.

NGC 6166, the brightest galaxy in the rich cluster Abell 2199, has been regarded as the classic multiple-nucleus galaxy since its original discussion by Minkowski (1961), and thus is a tempting first target for photometric decomposition. Minkowski identified four nuclei within the central $10h^{-1}$ kpc,

which he labeled A–D in order of decreasing luminosity. Minkowski also observed high velocities of nuclei B and C relative to A and calculated a mass-to-light ratio of $150h^{-1}$ for NGC 6166 under the assumption that the system was bound. Tonry (1984) reobserved the system and found B and C to have velocities of -1323 km s^{-1} and $+767 \text{ km s}^{-1}$ relative to A, respectively, while he measures only 280 km s^{-1} for the envelope velocity dispersion of galaxy A at the projected separations of B and C. Tonry concludes that B and C are not bound to A and are on radial orbits nearly along the line of sight; in this case the true separations of B and C from A could be much larger than their projected separations. This picture receives some support from Gregory and Thompson (1984) who measure 808 km s^{-1} as the line-of-sight velocity dispersion of galaxies in A2199. Lachièze-Rey, Vigroux, and Souvion (1985), hereafter LVS, presented an ad hoc decomposition of a CCD image of NGC 6166 and also conclude that B and C are not interacting with A and thus that the system is consistent with line-of-sight superposition of cluster galaxies.

This paper presents further decomposition of NGC 6166 with particular emphasis on the properties of the secondary nuclei and a search for low-contrast tidal distortions. The decomposition is done with a general multiple-isophote fitting algorithm which solves for the brightness distributions of all component galaxies simultaneously. LVS used a decomposition scheme based on recursively reflecting portions of galaxy A opposite its nucleus from B and C to estimate the background due to A under B and C. While this approach works for secondary galaxies well removed from the central galaxy, this author's experiments show it to become cumbersome and subject to error when several nuclei are present, occur on either side of the main galaxy, or have small separations from it. The present algorithm is developed as a first step to deal with the full range of complexity evident in a photometric survey of multiple-nucleus first-ranked galaxies (Lauer 1986).

II. OBSERVATIONS AND DECOMPOSITION

a) Observations

A 300 s exposure *g* band image of NGC 6166 was obtained by James E. Gunn, using the 4-SHOOTER CCD camera mounted at the Cassegrain focus of the Hale 5 m reflector. The signal-to-noise ratio per pixel in each nucleus was well in excess of 100 (this S/N ratio is reached at *g* surface brightness 19.65). The 4-SHOOTER camera uses four TI 800 × 800 pixel CCDs to image a large contiguous panoramic field. Each chip has a 0".334 per pixel scale which yields a 4.45 by 4.45 field. Since the present study concentrates on the center of NGC 6166, only one CCD was used. The seeing was 1".2 FWHM; however, interaction of the fast (*f*/1.8) camera optics with CCD thickness variations caused minor point-spread functions (PSF) width variations across the field.

Basic image reduction was carried out with VISTA (Lauer, Stover, and Terndrup 1983) installed under UNIX on Princeton University Observatory's VAX 11/750. Dome flat fields were sufficient to remove CCD sensitivity variations to 2%. Large-scale two-splines fitted to reduced night sky images were used to reduce these residual variations further to 0.5%. Sky levels were measured in each image corner by standard histogram techniques; the final sky level was the minimum of this

set and comes from an area 2.61 from the center of NGC 6166 at position angle 148°. A picture of the reduced image is presented in Figure 1 (Plate 2), and a contour map is presented in Figure 2. Photometric calibration is provided by Hoessel, Gunn, and Thuan (1980).

b) Decomposition of Composite Galaxy Systems

The decomposition of NGC 6166 is done by an algorithm developed for the general problem of analyzing a projected composite system of *N* galaxies. It is assumed here that the complex morphology of NGC 6166 results from line-of-sight superposition of normal ellipticals and a central CD. For simple superposition, the observed intensity, $I(x, y)$, at any pixel location x, y , is given by

$$I(x, y) = \sum_{n=1}^N G_n(x, y), \quad (1)$$

where $G_n(x, y)$ is the intensity contribution of galaxy *n* at that pixel. The problem is to recover the form of the individual galaxies given $I(x, y)$. This is done assuming only that the isophotes of the individual galaxies are concentric and elliptical in functional form. Both constraints are obeyed accurately in isolated elliptical galaxies (Lauer 1985a). Otherwise, the gal-

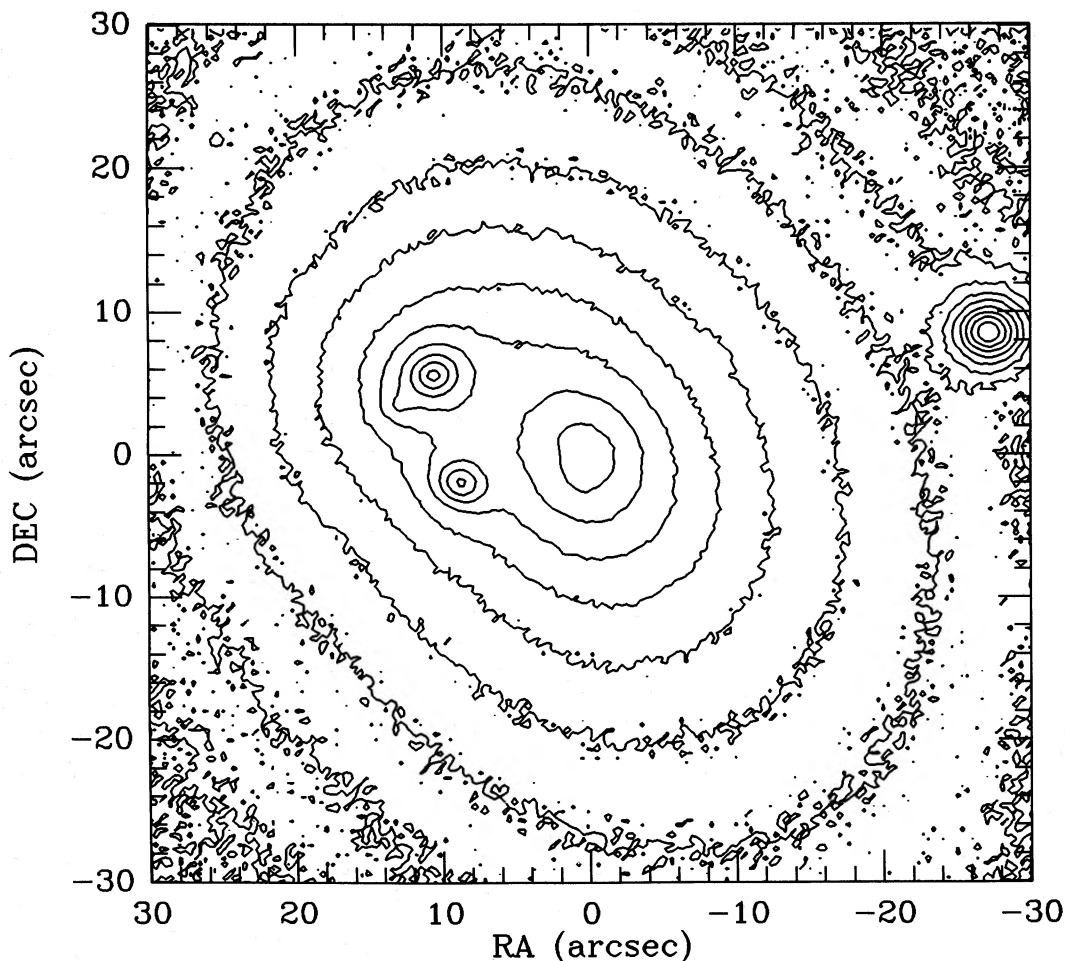


FIG. 2.—Contour map of NGC 6166. Contour levels are in 0.5 mag steps. The nucleus of galaxy A, the cD, is centered in the map; the innermost contour around its nucleus is at 19.5 mag arcsec⁻² in the *g* band. Galaxy B is to the northeast, and galaxy C is to the southeast. Nucleus D is visible a few arc seconds to the southeast of galaxy B's nucleus.

PLATE 2

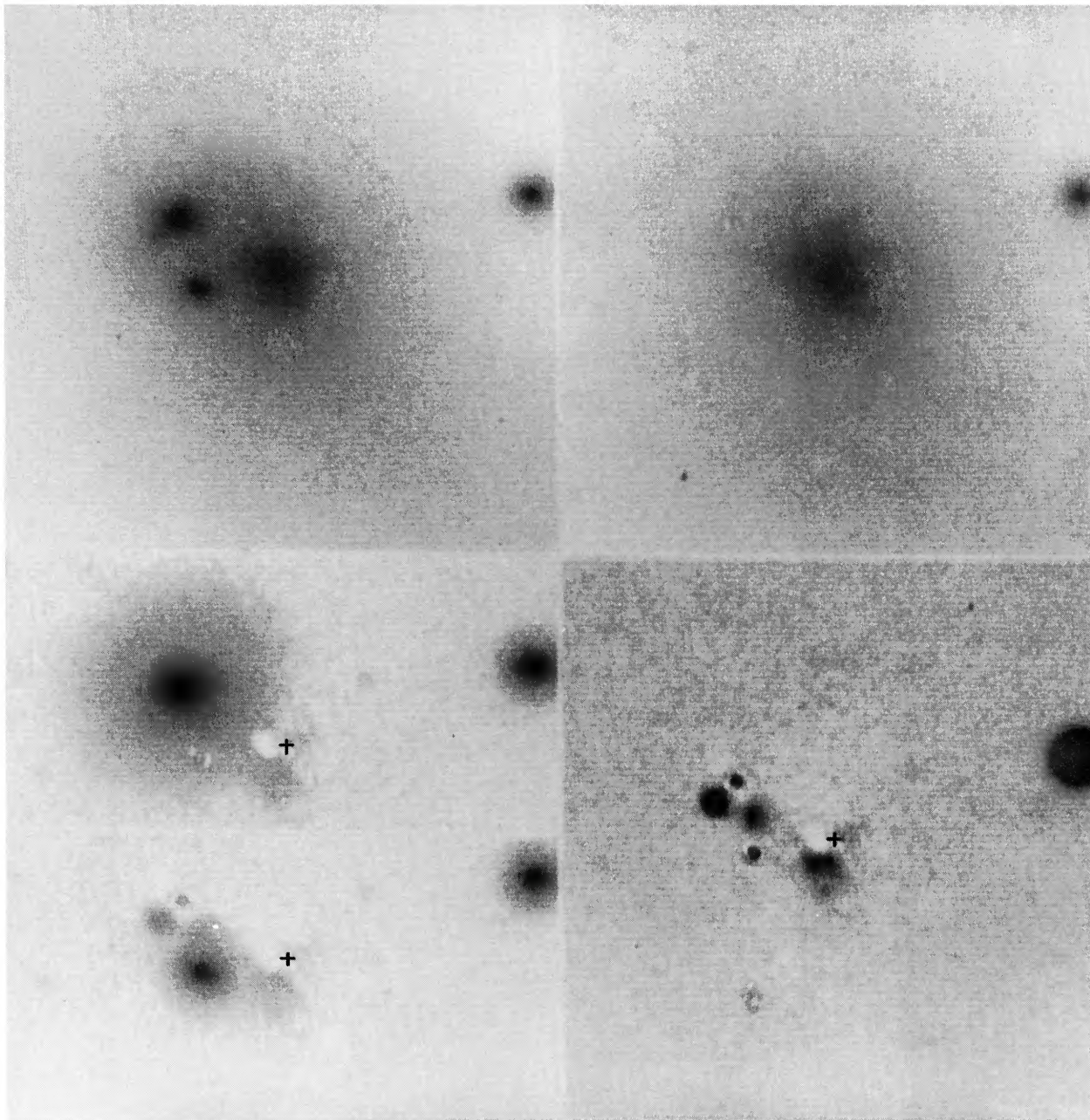


FIG. 1.—The upper left panel shows the central square arcminute of NGC 6166. Galaxies B and C and nucleus D are all visible to the east (north is to the top and east to the left in all panels). The upper right panel shows just the central cD galaxy after models of galaxies B and C have been subtracted. Nucleus D has also been removed. Model-fitted residuals are still visible at the central positions of galaxies B and C. Galaxies B and C are seen in isolation in the upper and lower halves of the lower left panel; crosses mark the central position of the cD. Nucleus D has been removed from the image of galaxy B but is left behind in the image of galaxy C. The lower right panel shows a highly stretched image of the residuals left behind after models of galaxies A, B, and C were subtracted from the original image.

LAUER (see page 35)

axes are allowed to have arbitrary isophote brightness, ellipticity, and position angle profiles to account for the wide variety of brightness distributions, shapes, and isophote twistings seen in normal elliptical galaxies (see Kormendy 1982). This approach also allows for some plausible interaction effects between the galaxies despite the pure projection assumption; any isophote twisting, symmetric stretching, or truncation of the infalling ellipticals produced by tidal interaction with the central cD should be recovered. Further, the projection hypothesis is tested directly by comparing the "best-fit" superposition model to the original image. Asymmetrical distortions of the isophotes, tidal tails, or any other structures not encompassed by the model should be readily visible.

The form of each galaxy is thus specified by its set of K_n isophotes. The major-axis lengths, a_k , of the isophotes are specified in advance and have the same values for each galaxy. The free parameters for each isophote are its surface brightness, μ_{nk} , ellipticity, ϵ_{nk} , and position angle, ϕ_{nk} , which are found by a nonlinear least-squares isophote fitting algorithm similar to that presented by Willims and Schwarzschild (1979). The algorithm proceeds by iteratively fitting estimates of the galaxy forms to the image with first-order terms to account for parameter errors. At any stage, the contribution of galaxy n to any pixel is found by interpolating between the isophotes bracketing the pixel, given the distance, r_n , and position angle, θ_n , of the pixel from the nucleus position, x_n, y_n , where

$$r_n = [(x - x_n)^2 + (y - y_n)^2]^{1/2}, \quad (2)$$

and

$$\theta_n = \tan^{-1} \frac{y - y_n}{x - x_n}. \quad (3)$$

The distances to the bracketing isophotes k and $k+1$ are found such that $d_{nk} < r_n < d_{nk+1}$, where

$$d_{nk} = a_k(1 - \epsilon_{nk})[\sin^2(\phi_{nk} - \theta_n) + (1 - \epsilon_{nk})^2 \cos^2(\phi_{nk} - \theta_n)]^{-1/2}. \quad (4)$$

The intensity of the galaxy is then calculated by logarithmic interpolation:

$$G_n(x, y) = \mu_{nk} \left(\frac{r_n}{d_{nk}} \right)^\gamma, \quad (5)$$

where

$$\gamma = \log \left(\frac{\mu_{nk+1}}{\mu_{nk}} \right) / \log \left(\frac{d_{nk+1}}{d_{nk}} \right). \quad (6)$$

This method of interpolation is highly accurate, except in the inner $1''$ of the nuclei where the curvature of the luminosity profiles can be strong. Since residuals here are highly localized and have zero sum, however, they do not affect isophotes of neighboring galaxies. Six first-order terms are also calculated, $\partial G_n / \partial \mu_{nk}$, $\partial G_n / \partial \epsilon_{nk}$, $\partial G_n / \partial \phi_{nk}$, (and the same terms of the $k+1$ isophote) which are used to compute corrections to the isophote parameters, $\Delta \mu_{nk}$, $\Delta \epsilon_{nk}$, $\Delta \phi_{nk}$, by the inversion of

$$\begin{aligned} \sum_{x,y} \sigma_{x,y}^{-2} \left[I(x,y) - \sum_{n=1}^N G_n(x,y) \right] \\ = \sum_{x,y} \sigma_{x,y}^{-2} \sum_{n=1}^N \sum_{j=k(n)}^{k(n)+1} \sum_{i=1}^3 \frac{\partial G_n(x,y)}{\partial p_{nji}} \Delta p_{nji}, \quad (7) \end{aligned}$$

where p_{nji} represents the three isophote k parameters of galaxy n and $\sigma_{x,y}$ is the expected error in $I(x,y)$.

In the present application $\sigma_{x,y}$ is calculated for each pixel on the assumption that shot noise is the only source of random errors in the pixel values; this means that the decomposition procedure requires knowledge of the sky level (although eq. [7] assumes prior subtraction of the sky from $I(x,y)$ itself). Since each pixel is normalized by its expected error, bright pixels in the cores of the galaxies do not bias the decomposition; there is no *a priori* difficulty in solving for the outer isophotes of a galaxy that may overlap with or even encompass the bright central regions of other galaxies in the image, provided that its isophotes contribute significantly to pixels at least elsewhere in the image. The error in the solution for any isophote parameter is based on its contribution to the χ^2 value of the model residuals; the relative error in the parameter increases as the parameter's significance to the solution decreases. In practice, loss of significance determines the limiting radius for the solution of an individual galaxy's image rather than any explicit constraints imposed by the complexity of the multiple galaxy system.

III. RESULTS

a) Morphology

The three main galaxies, A, B, and C were entered into the isophote fitting algorithm. Isophotes for each galaxy were centered on its nucleus centroid. Pixels around nucleus D and in two other regions discussed below were ignored in the fit. Contour maps of the individual galaxies with the fits of the other galaxies subtracted off are shown in Figures 3–5. Individual images of the component galaxies are also shown in Figure 1, as well as a map of the composite fitted residuals.

The assumption that NGC 6166 can be explained by superposition works well. The isophotes of all three galaxies appear to be concentric and show no global distortion or shear away from their elliptical forms. Nonconcentric isophotes, for example, cause the residuals to form dipole patterns about the nuclei; no such patterns are seen here. Nevertheless, a number of features are visible in the residual map. Dust absorption in galaxy A's nucleus, noted by Minkowski (1961) and Burbidge (1962), shows up here as a complex pattern of residuals in Figure 1. A narrow dust lane runs south of the nucleus, with a deeper cloud of absorption to its northwest (pixels affected by dust were excluded from the fit). The amount of absorption is ~ 0.15 magnitudes in the deepest parts of the dust lane, although this estimate should be regarded as uncertain due to seeing effects. There may be more dust absorption north of the nucleus. Large negative residuals are seen in this area, with large positive residuals to the south. Although this residual pattern superficially resembles the effects of nonconcentric isophotes, the localized nature of the residuals suggests more that the isophotes near the center have been disturbed by dust absorption. None of the residuals are likely to be due to gas emission since no extended H II emission was seen in this galaxy by Cowie *et al.* (1983). Galaxy A does show [O II] in emission but only in an unresolved nuclear component (Minkowski 1961). The unresolved cores of B and C are poorly sampled by the isophote grid, as noted above in § IIB; core residuals are clearly visible in Figures 1–5 where galaxies B and C have been subtracted. Nucleus D shows no extended emission and appears to be stellar in morphology; its apparent g magnitude is 19.8. If it is a cluster galaxy, it would have to be strongly truncated. Last, an elongated feature is seen along the line connecting galaxies B and C (the pixels around this object

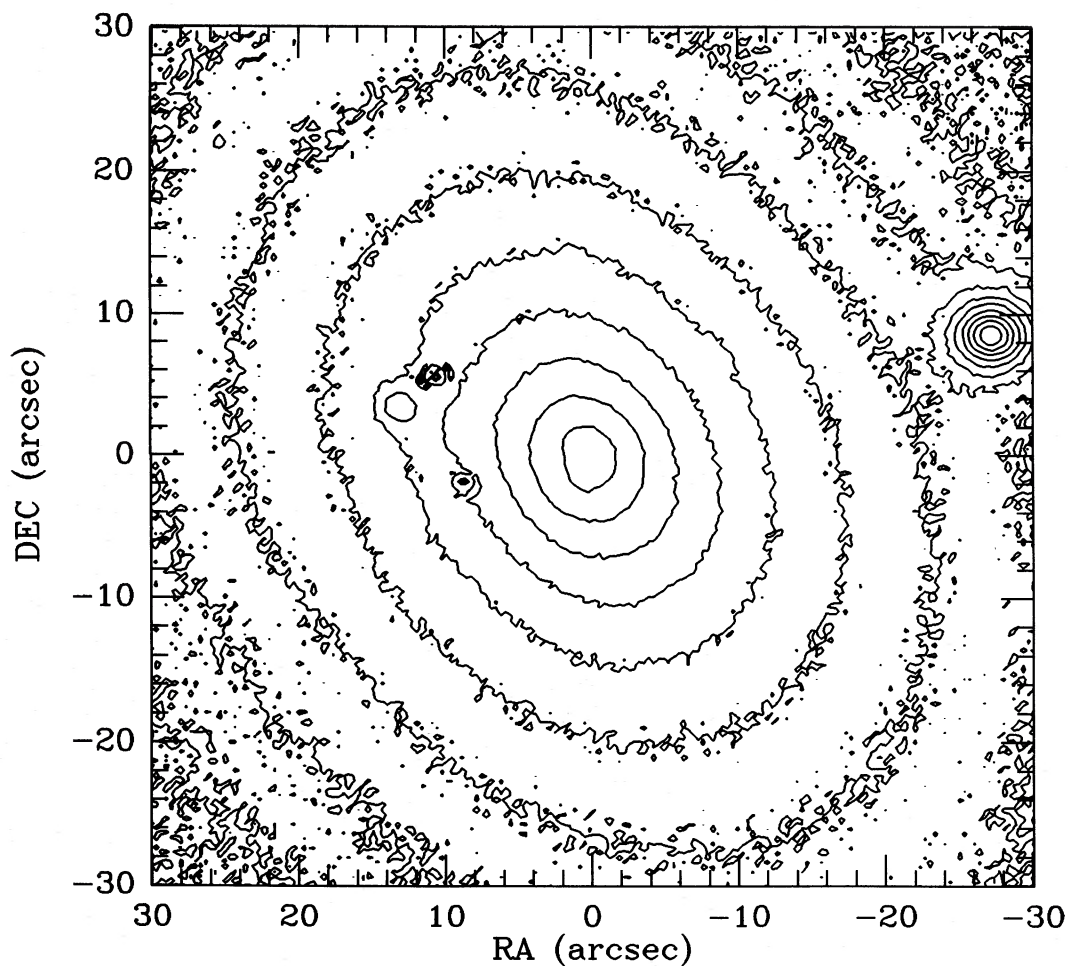


FIG. 3.—Models of galaxies B and C have been subtracted from the original image of NGC 6166, leaving behind an image of just the central cD galaxy, NGC 6166A. Contour levels are as in Fig. 2. Large residuals in the model fitted to the nuclei of galaxies B and C are visible to the east, as is nucleus D.

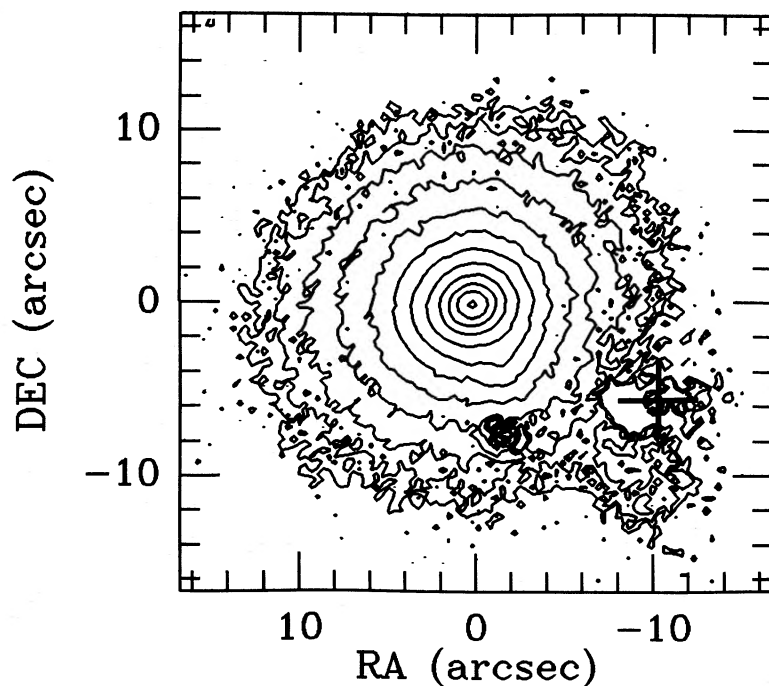


FIG. 4.—Contour map of NGC 6166B, obtained by subtracting models of galaxies A and C and clipping out nucleus D from the original image. The outermost contour is at $24.0 \text{ mag arcsec}^{-2}$ in the g band. Nuclear residuals mark the center of galaxy C, and a plus sign (+) marks the center of galaxy A.

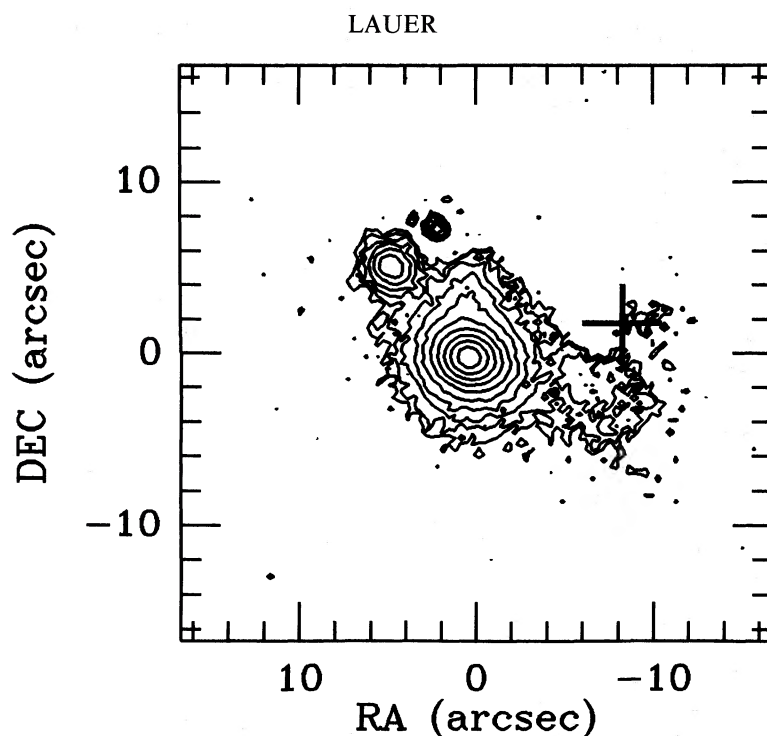


FIG. 5.—Contour map of NGC 6166C, obtained by subtracting models of galaxies A and B from the original image. The outermost contour is at $24.0 \text{ mag arcsec}^{-2}$ in the g band. Nuclear residuals mark the center of galaxy B, and a plus sign (+) marks the center of galaxy A. Nucleus D is to the northeast, and a faint elongated feature positioned between galaxies B and C is to the north.

were ignored in the fit). This feature is faintly visible in Burbidge (1962) and is also seen by J. Kormendy (private communication) under excellent seeing conditions. It is centrally condensed, and its surface brightness drops off before reaching into the nucleus of either galaxy. Its apparent g magnitude is 20.6. The feature may be a dynamical friction wake induced by the passage of galaxy C through the cD (the major axis of the feature points straight at the nucleus of galaxy C). Similar features are seen in other multiple systems with clearly interacting galaxies (Lauer 1986). Further, the morphology and orientation of the feature strongly resemble wakes observed in theoretical studies of orbital decay of satellite galaxies around more massive galaxies (Weinberg 1986). If this picture is correct, then the wake contains information on the total velocity vector of galaxy C and its de-acceleration by the cD.

b) Surface Photometry

Surface photometry profiles of galaxies A, B, and C are presented in Figures 6–8. For the most part, the profiles verify the above results, namely, that the galaxies individually appear to be morphologically normal elliptical galaxies. The central galaxy A has a simple de Vaucouleurs law surface brightness profile over the region of interest, which flattens off to a well-resolved core near the center. As first noted by Kormendy (1985a), the core profile is isothermal unlike the case for normal elliptical galaxies (Lauer 1985b). The isophotes show no twisting but do increase in ellipticity with radius.

The brightness profile for galaxy B appears to be a truncated de Vaucouleurs law; the implied truncation radius is $22''$. The truncation is also visible in the contour plot in Figure 4, which shows the close spacing of the outer isophotes at all position angles. This truncation is quite strong; the profile falls off too steeply to be explained as a superposition of a bulge and disk system, which can mimic truncated profiles in logarithmic

coordinates. The truncation has been noted before by LVS and may be evidence for interaction of galaxy B with the central cD; the present profile agrees well with that of LVS. The obvious question is whether the strong background from galaxy A has been subtracted out properly. The last two isophotes measured in galaxy B fall ~ 2.5 and 3.5 mag below the median background from galaxy A. The same isophotes fall 0.5 and 1.4 mag below a de Vaucouleurs law profile defined by the inner isophotes. Tests on simulated systems show that random errors in the brightness profiles are still small at these contrast levels. Figure 9 shows the results of a simulation designed to match the geometry, structure, and noise of the composite galaxy A plus B system on the assumption that both really follow normal de Vaucouleurs profiles. As can be seen, a normal untruncated de Vaucouleurs profile is recovered for galaxy B. Systematic errors from residual CCD sensitivity variations are more important, but even here they are expected to be too small to explain the truncation. Even if the nominal 0.5% residual sensitivity variations occurred over the small extent of the image analyzed, which is unlikely, then errors in the outer two isophotes should still be limited to 0.15 and 0.50 mag ; if galaxy B really had an untruncated de Vaucouleurs law, then errors in the same isophotes would be only 0.09 and 0.16 mag . The image of galaxy B is round and undistorted despite the strong background gradient from galaxy A. The isophotes may twist slightly away from the separation vector between galaxy B and the cD; the average major axis position angle with respect to this vector is 80° (systematic errors in the outermost isophote can easily account for its apparently discrepant position angle). In short, it appears that the subtraction worked well and the galaxy is truly truncated.

Last, galaxy C appears to have a normal but steeply falling de Vaucouleurs law profile. Its isophotes become increasingly elongated with radius but show little evidence of twisting. As

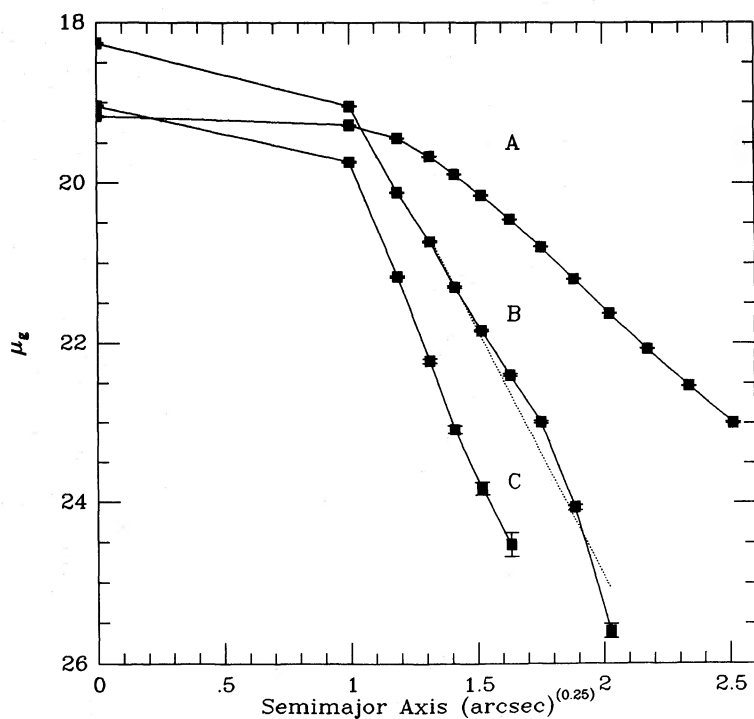


FIG. 6.—Surface photometry in the g band for galaxies A, B, and C as a function of isophote semimajor axis length to the 0.25 power. A dashed line shows the de Vaucouleurs law fitted to galaxy B.

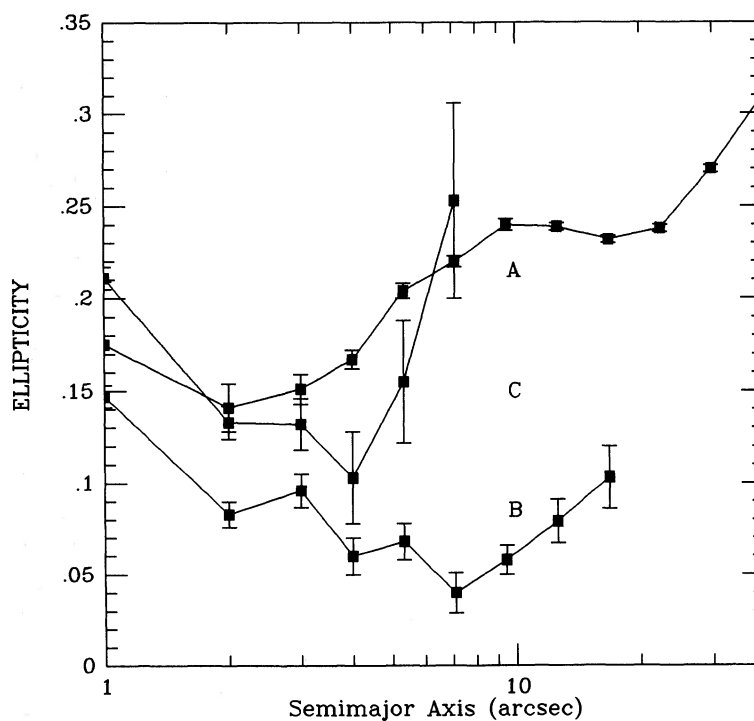


FIG. 7.—Isophote ellipticity profiles for galaxies A, B, and C

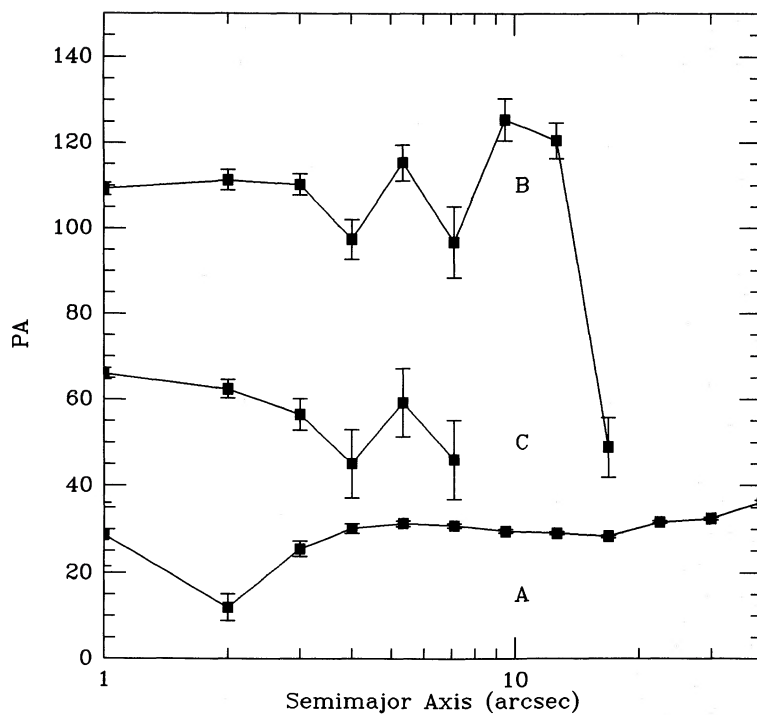


FIG. 8.—Isophote position angle profiles for galaxies A, B, and C

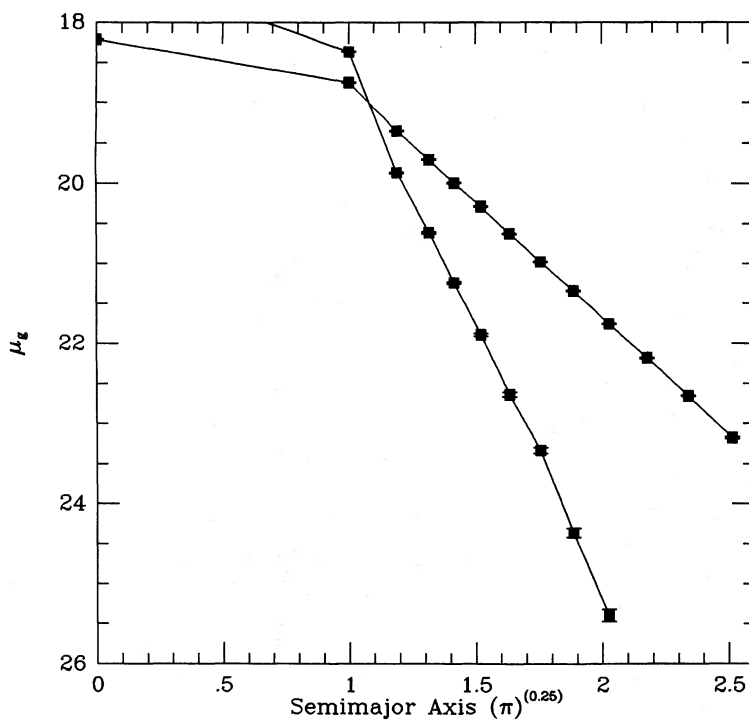


FIG. 9.—A test of the decomposition procedure on a simulated image matching the geometry, structure (but with galaxy C excluded), and noise of the observed image system under the assumption that both galaxies A and B have untruncated de Vaucouleurs surface brightness profiles. The decomposition procedure is able to recover the input g band surface photometry profiles for both galaxies.

TABLE 1
NGC 6166 COMPONENT GALAXY PARAMETERS

Galaxy	R_{sep} (kpc)	P.A.	m_B	M_B	R_E (kpc)	I_E	r_C (pc)	I_0	M/L_B
A.....	12.51	-23.55	45	24.88	3030	19.20	6.3
B.....	8.4	61.4	15.96	-20.10	2.3	21.55	<350	<17.10	3.1
C.....	6.2	102.2	17.73	-18.33	0.75	20.61	<350	<17.80	4.4

NOTE.—Distance-dependent parameters assume $H_0 = 60 \text{ km s}^{-1} \text{ Mpc}^{-1}$. Mass-to-light ratios are in solar units.

with galaxy B, if anything, the major axis twists away from rather than toward alignment with the projected galaxy-cD separation vector; the average position angle of the major axis with respect to this vector is 50° .

c) Measured Parameters

Luminosities, effective radii, and other characteristic parameters of the galaxies constituting NGC 6166 are presented in Table 1 for comparison to those of normal isolated galaxies. For convenience, all parameters are transformed to the B band assuming $B - g = 0.68$ (Schneider, Gunn, and Hoessel 1983b). Effective radii and surface brightnesses were measured by de Vaucouleurs law fits to the profiles outside the central $3''$ to avoid seeing effects; the small R_e values for galaxies B and C simply reflect the steep falloff of their envelopes. Apparent magnitudes for the galaxies were calculated from the R_e and I_e values, and direct integration of the light within the central $3''$. A fit to just the inner nontruncated portion of galaxy B's profile gives an effective radius of 5.1 kpc, which is over twice as large as the present value; a luminosity calculated from this fit is 0.36 mag brighter than the value given in Table 1. The present apparent magnitudes are in excellent agreement with those of previous investigators. Oemler (1976) gives $m_B = 12.49$ for galaxy A. LPV calculate m_B for galaxies B and C as 16.05 and 17.90, respectively. Absolute magnitudes were calculated with $H_0 = 60 \text{ km s}^{-1} \text{ Mpc}^{-1}$ and $q_0 = 0.5$ using $z = 0.0312$ (Hoessel, Gunn, and Thuan 1980). A g band K correction of 0.08 mag has been applied (Schneider, Gunn, and Hoessel 1983b); extinction for this system is negligible (Burstein and Heiles 1984).

Galaxy core parameters are also presented in Table 1. These are derived from profiles with much finer isophote spacing than those presented above. Only galaxy A has a core large enough to be resolved under the present seeing conditions. The cores of galaxies B and C are severely unresolved; upper limits are given for their core parameters based on model seeing-convolutions presented by Schweizer (1981), but their true values are most likely much smaller (Lauer 1985b). Mass-to-light ratios are calculated from the standard isothermal core formula (King and Minkowski 1972), using the present core parameters and velocity dispersions measured by Tonry (1984). The mass-to-light ratios are not as strongly affected by seeing as r_c and I_0 are individually; however, they should still be regarded as uncertain for galaxies B and C.

IV. DISCUSSION

The present success at modeling the structure of NGC 6166 as simple line-of-sight projection of two normal elliptical galaxies against a central cD galaxy offers constraints on plausible forms of physical interaction between the galaxies. Tonry (1984) has already argued that the relatively low 280 km s^{-1}

envelope velocity dispersion of galaxy A in comparison to the high radial velocities of galaxies B and C means that neither galaxy is bound to and thus presently merging with the cD; as argued below, the present results are consistent with this. A more difficult question is whether the orbits of galaxy B or C still carry them through the envelope of the cD or stay well away from it. In the former case, the galaxies would be subject to tidal shocks which might cause slow erosion of their envelopes by tidal stripping, a potentially important process for growth of the cD envelope (Richstone 1976). Simple calculations suggest that tidal shocks might produce recognizable effects on the infalling galaxies even during the short time they spend near their orbital pericenters. As an infalling galaxy travels though the cD at distance r from its center, stars within the infalling galaxy are subject to a differential tidal acceleration produced by the cD along the vector separating the two galaxies. To first order for an isothermal galaxy (a good approximation to galaxy A over the region of interest), the tidal acceleration of a star in the infalling galaxy relative to its center is

$$\ddot{r} = \frac{V_C^2}{r^2} d, \quad (8)$$

where V_C is the circular orbital velocity in the cD, and d is the distance of the star from the center of the infalling galaxy projected onto the galaxy-cD separation vector.¹ If the velocity of the infalling galaxy is large compared to its internal velocity dispersion σ , its stars receive an impulsive velocity change Δv , which can be calculated by integrating equation (8) over the galaxy's path through the cD. Under the present conditions, with the infall velocity $V \gg V_C$, it may be assumed that the orbital path is a straight line through the cD with an impact parameter a . Under these conditions, then

$$\Delta v = \frac{2V_C^2}{V} \left(\frac{d}{a} \right). \quad (9)$$

Most of Δv is received near closest approach—the impulse approximation appears good for $d > a\sigma/V$. The velocity impulse gives rise to spatial distortions of the galaxy, Δx , which to first order cause symmetrical twisting and elongation of its isophotes. Equation (8) integrated over $T = 2a/V$ centered on the time of closest approach gives

$$\frac{\Delta x}{d} \approx 2^{3/2} \left(\frac{V_C}{V} \right)^2. \quad (10)$$

Also of interest are second-order tidal effects, which produce

¹ This analysis ignores tidal forces perpendicular to the separation vector, which to first order average to zero over the encounter.

asymmetrical shear of the isophotes. Over the time of closest approach defined above, second-order distortions will grow as

$$\frac{\Delta x}{d} \approx 2.6 \left(\frac{V_C}{V} \right)^2 \left(\frac{d}{a} \right). \quad (11)$$

As Δv approaches σ , stars will be stripped from infalling galaxy's outer envelope, which leads to the definition of a tidal radius, R_T , from equation (9) as

$$R_T \approx \frac{a}{2} \left(\frac{\sigma V}{V_C^2} \right). \quad (12)$$

This is in contrast to $R_T \approx a\sigma/V_C$ for an isothermal galaxy in circular orbit around the cD. The effects of tides at the same impact parameter are much stronger here than they are for a galaxy which quickly passes through the cD.

The best limits on tidal shocks endured by galaxies B and C may be set by the shape of their luminosity profiles. As noted in § IIIb, galaxy B has a truncated profile with $R_T \approx 17$ kpc; from equation (12), this implies a previous close approach of ~ 20 kpc.² If the normal de Vaucouleurs profile of galaxy C implies that it has not been tidally truncated, then limits from the present photometry give $R_T > 5$ kpc, which gives a lower limit of 13 kpc for any previous impact parameter. Note that if either galaxy were on a nearly circular orbit as might occur during a merger, they would have to remain at larger radii still to escape damage by strong tidal effects.

There is also little evidence from the morphologies of either galaxy B or C to suggest recent encounters (but longer than $T = a/V$ or $\sim 10^7$ yr ago) with galaxy A at distances much smaller than the limits given above. If it is assumed that their observed radial velocities of 1323 and 767 km s⁻¹ relative to the cD are close to their true orbital velocities (which may be a fair assumption for galaxy B since the line-of-sight velocity dispersion in A2199 is only 808 km s⁻¹), and taking $V_C \approx 1.4\sigma$ or 390 km s⁻¹ for galaxy A, then the first- and second-order values of $\Delta x/d$ are 0.25 and 0.24(d/a) for galaxy B and 0.73 and 0.67(d/a) for galaxy C. These terms are large enough to produce readily visible isophote stretching and twisting. Interestingly, galaxy C is strongly elongated and becomes more so with radius. In contrast, galaxy B is nearly circular, with isophotes becoming no more elliptical than 10%. No strong isophote twisting is seen in either galaxy, however, if anything, the isophotes twist slightly away from rather than toward the cD as would be expected. Although this may reflect unfavorable geometry or initial conditions, it also makes it difficult to show that either galaxy is not an undisturbed elliptical, which can often have a similar isophote ellipticity profile (Lauer 1985c). Further, for the small values of a under consideration, of order 10 kpc or so, effects of the asymmetric second-order terms should also be readily detectable, given the steep luminosity profiles of both galaxies. The most interesting constraints on the *present* locations of galaxies B or C relative to the cD may come from the presence or absence of dynamical friction wakes in the cD envelope induced by their passage through it. If the faint feature associated with galaxy C discussed in § IIIb is such a wake, then of course galaxy C must be presently embedded in the cD galaxy, even if it is not as close to the CD nucleus as its projected distance.

² Tonry's (1984) measurement of a steeply falling dispersion profile in this galaxy may also be evidence of envelope truncation; with the "lid" lifted off, stars remaining in the envelope may have a radially anisotropic velocity ellipsoid.

Of course, the above arguments on the growth of tidal distortions depend strongly on the epoch of closest approach; the fiducial time $T = 2a/V$ was only chosen to explore growth of tidal effects while the galaxies remain close to the center of the cD. Tidal distortions, for example, would be small and probably undetectable before closest approach; on the other hand, they can continue to grow until well after this time provided internal orbital motions in the infalling galaxy remain unimportant, or at a given radius until time $T \approx d/\sigma$.

It also appears that any ongoing tidal erosion of galaxies B and C could only be in early stages since both galaxies appear to have normal dispersions, cores, and effective radii for their luminosities. As tidal erosion occurs, for example, a galaxy's nuclear velocity dispersion should remain unchanged as its envelope is stripped off; stripped galaxies should have excessive dispersions for their *present* luminosities when compared to the Faber-Jackson (1976) relationship for normal ellipticals. The velocity dispersions measured by Tonry (1984) for all three galaxies in NGC 6166 are plotted against their magnitudes in Figure 10 along with the Faber-Jackson relationship derived by Tonry and Davis (1982) for normal ellipticals. As can be seen, galaxy A has an abnormally low dispersion for its luminosity, which appears to be a general property of cD galaxies (Malumuth and Kirshner 1981). Galaxies B and C, however, appear to have normal dispersions within the uncertainties of measuring errors and intrinsic scatter in the Faber-Jackson relation (which admittedly makes this only a test of strong tidal stripping). Galaxies B and C have unresolved cores which offer little constraint on their central structure. Nevertheless, the present limits on core parameters are compatible with galaxies of B and C's luminosities; their low central mass-to-light ratios may indicate that their cores are much denser still (Lauer 1985b). Stripped galaxies should also appear compact for their luminosity since tidal ablation removes loosely bound stars at large radii first. Figure 11 shows that while both galaxies B and C are compact when compared to the magnitude-radius relationship derived for normal elliptical galaxies (Lauer

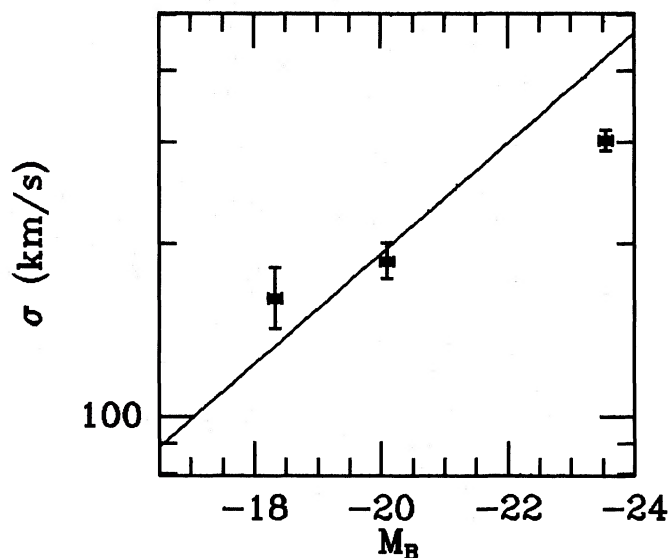


FIG. 10.—Nuclear velocity dispersion as a function of luminosity for galaxies A, B, and C. Dispersions are taken from Tonry (1984). The solid line is the Faber-Jackson relationship for elliptical galaxies measured by Tonry and Davis (1981).

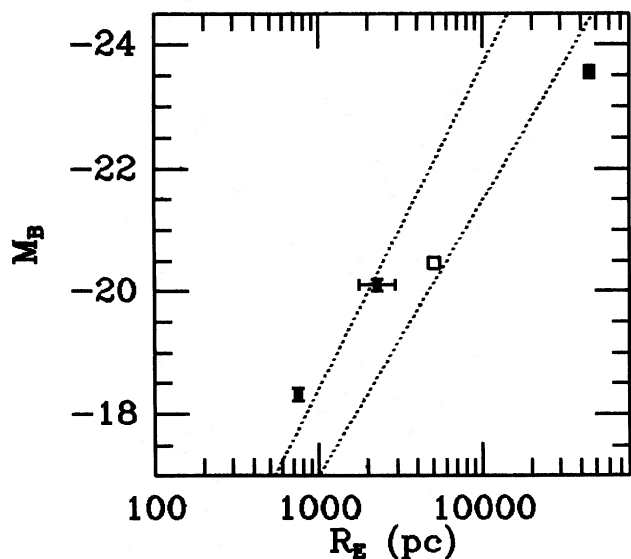


FIG. 11.—The magnitude-radius relationship for galaxies A, B, and C. The line to the left is the magnitude-radius relationship for galaxies in the inner 1 Mpc of A2199 measured by Strom and Strom (1978), while the line to the right is that for normal elliptical galaxies (Lauer 1985b). The open square marks the position of galaxy B in this diagram based on a fit to the portion of its profile unaffected by truncation.

1985b), both are normal when compared to the relationship measured by Strom and Strom (1978) for galaxies in the central 1 Mpc of A2199; these investigators have shown in several cases that galaxies in the cores of rich clusters are more compact than those in the cluster outskirts. In other words, while B and C may have undergone tidal stripping by the cD in the past, they are not unusual in this regard when compared to galaxies in the core of A2199 presently well removed from the cD. Note that the inner profile of galaxy B may reflect the original state of the galaxy; a luminosity and effective radius calculated from the inner profile plotted in Figure 11 falls much closer to the normal magnitude-radius relationship.

V. CONCLUSION

NGC 6166 was modeled as the superposition of a central cD, galaxy A, and two low-luminosity elliptical galaxies, B and C. Surface photometry was derived for each of these galaxies by a simultaneous isophote algorithm under the assumption that the morphology of NGC 6166 results from simple line-of-sight superposition of galaxies that have concentric elliptical isophotes but otherwise arbitrary brightness, position angle, and ellipticity profiles. Subtraction of model images of A, B, and C from the original image leaves a smooth residual image.

The nuclear dust clouds in galaxy A noted by Burbidge (1962) are clearly visible, nucleus D noted by Minkowski (1961) appears stellar, and a faint narrow feature is observed between galaxies B and C, which may be a dynamical friction wake in the envelope of the cD induced by the passage of galaxy C; there is no other evidence for any faint tidal plumes or any diffuse structures that might indicate mutual interaction between the component galaxies. The success of the model fit verifies the assumption that each galaxy has concentric elliptical isophotes unaltered by tidal shear, tidal tails, or any other asymmetric distortions; a conclusion that has also been reached by Lachièze-Rey, Vigroux, and Souviron (1985) through their own photometric analysis.

Tonry's (1984) dynamics observations indicate that neither galaxy B or C are bound to the cD but still may be free to pass rapidly through its envelope. In this case tidal shocks may still produce recognizable distortions of the galaxies closely after their time of closest passage to the cD even though the strong tidal effects of a merging encounter may be avoided. The luminosity profile of galaxy B is truncated, which may indicate a previous close approach of 20 kpc to the cD and galaxy C may be presently passing through the envelope of the cD if the faint feature noted above is a dynamical friction induced wake; however, neither galaxy shows the strong truncation that would be expected if they have passed as close to the center of the cD as their projected radii. The lack of asymmetric distortions or strong isophote twisting in either galaxy also supports the conclusion that neither galaxy has recently passed within ~ 10 kpc of the center of the cD.

Galaxies B and C cannot have suffered from extreme tidal stripping as might be seen in the final stages of a merger since both galaxies also have normal velocity dispersions for their luminosities. Nevertheless, in addition to the truncated profile of galaxy B, some level of tidal stripping by the cD is indicated since galaxies B and C are both compact for their luminosity when compared to normal elliptical galaxies; however, neither galaxy is unusual in this regard when compared to the magnitude-radius relationship measured by Strom and Strom (1978) for other galaxies in the inner 1 Mpc of A2199. In short galaxies B and C appear to be normal members of the core population of A2199. Their orbits may occasionally carry them through the cD, but they do not appear to be the surviving cores of much more luminous galaxies strongly cannibalized by the cD.

I wish to thank Jim Gunn for the observations and useful conversations. I am also grateful to Jerry Ostriker and Barbara Ryden for useful conversations. This work was supported by NSF grant AST84-20532.

REFERENCES

- Burbidge, E. M. 1962, *Ap. J.*, **136**, 1134.
 Burstein, D., and Heiles, C. E. 1984, *Ap. J. Suppl.*, **54**, 33.
 Cowie, L. L., Hu, E. M., Jenkins, E. B., and York, D. G. 1983, *Ap. J.*, **272**, 29.
 Faber, S. M., and Jackson, R. E. 1976, *Ap. J.*, **204**, 668.
 Gregory, S. A., and Thompson, L. A. 1984, *Ap. J.*, **286**, 422.
 Hausman, M., and Ostriker, J. P. 1978, *Ap. J.*, **224**, 320.
 Hoessel, J. G. 1980, *Ap. J.*, **241**, 493.
 Hoessel, J. G., Gunn, J. E., and Thuan, T. X. 1980, *Ap. J.*, **241**, 486.
 King, I. R., and Minkowski, R. 1972, in *IAU Symposium 44, External Galaxies and Quasi-Stellar Objects*, ed. D. S. Evans (Dordrecht: Reidel), p. 87.
 Kormendy, J. 1982, in *Morphology and Dynamics of Galaxies*, ed. L. Martinet and M. Mayor (Sauvigny: Geneva Observatory), p. 113.
 Kormendy, J. 1985, *Ap. J. (Letters)*, **292**, L9.
 Lauer, T. R. 1985a, *M.N.R.A.S.*, **216**, 429.
 ———. 1985b, *Ap. J.*, **292**, 104.
 ———. 1985c, *Ap. J. Suppl.*, **57**, 473.
 ———. 1986, in preparation.
 Lauer, T. R., Stover, R. J., and Terndrup, D. M. 1983, *The VISTA User's Guide* (Lick Observatory Tech. Rept. No. 34).
 Lachièze-Rey, M., Vigroux, L., and Souviron, J. 1985, *Astr. Ap.*, **150**, 62 (LVS).
 Malumuth, E. L., and Kirshner, R. P. 1981, *Ap. J.*, **251**, 508.
 Merritt, D. 1984a, *Ap. J.*, **276**, 26.
 ———. 1984b, *Ap. J. (Letters)*, **280**, L5.
 Minkowski, R. P. 1961, *A.J.*, **66**, 558.

- Oemler, A. 1976, *Ap. J.*, **209**, 693.
Richstone, D. O. 1976, *Ap. J.*, **204**, 642.
Schneider, D. P., Gunn, J. E., and Hoessel, J. G. 1983*a*, *Ap. J.*, **268**, 476.
———. 1983*b*, *Ap. J.*, **264**, 337.
Schweizer, F. 1981, *A.J.*, **86**, 662.
Strom, K. M., and Strom, S. E. 1978, *A.J.*, **83**, 1293.
- Tonry, J. L. 1984, *Ap. J.*, **279**, 13.
———. 1985, *Ap. J.*, **291**, 45.
Tonry, J. L., and Davis, M. 1981, *Ap. J.*, **246**, 680.
Weinberg, M. D. 1986, *Ap. J.*, **300**, 93.
Williams, T. B., and Schwarzschild, M. 1979, *Ap. J.*, **195**, 156.

TOD R. LAUER: Princeton University Observatory, Peyton Hall, Princeton, NJ 08544